



Probing the nature of electroweak symmetry breaking with Higgs boson pairs in ATLAS

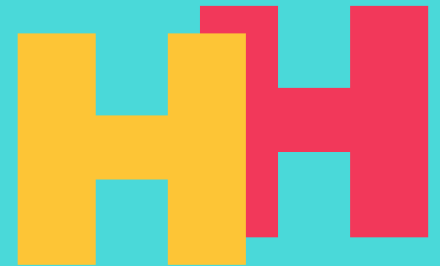
Shahzad Ali, Cal State University East Bay, US

On behalf of ATLAS collaboration

31st International Workshop on Deep Inelastic Scattering



8–12 April 2024



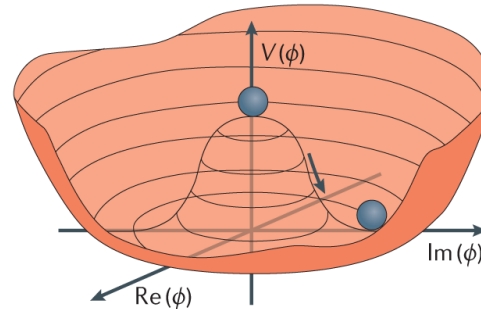
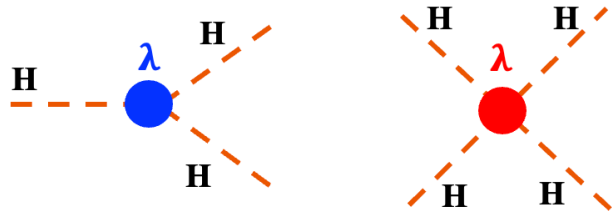
Higgs self-coupling (Physis Motivation)

- The full expression of the Higgs potential is encoded with parameters μ and λ as:

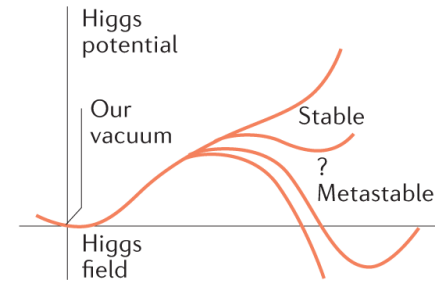
$$V(\phi) = \mu^2(\phi^\dagger\phi) + \lambda(\phi^\dagger\phi)^2$$

- When linearising the Higgs field after the EWSB around the vacuum expected value v one gets:

$$V(H) = \frac{1}{2}m_H^2 H^2 + \lambda v H^3 + \frac{\lambda}{4} H^4 - \frac{\lambda}{4} v^4 \quad \lambda_{HHH} = \lambda_{HHHH} = \frac{m_H^2}{2v} \approx 0.13 \rightarrow \text{SM prediction}$$



Nature reviews physics



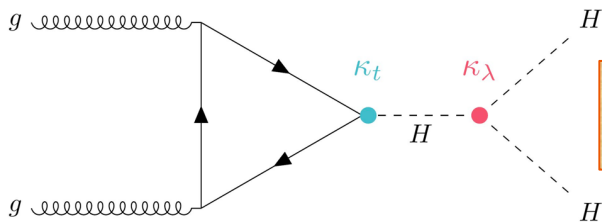
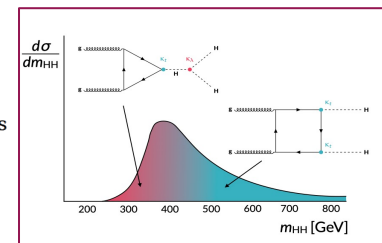
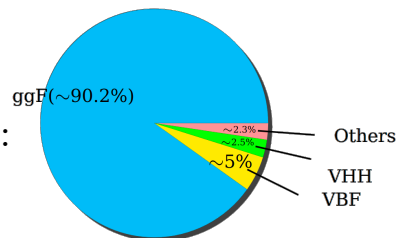
- Investigating the HH production allows for direct probing of the Higgs self-coupling
 - One of the unknown property after the Higgs discovery still to be measure
 - Prob the shape of the Higgs potential

Higgs self coupling measurements at the LHC

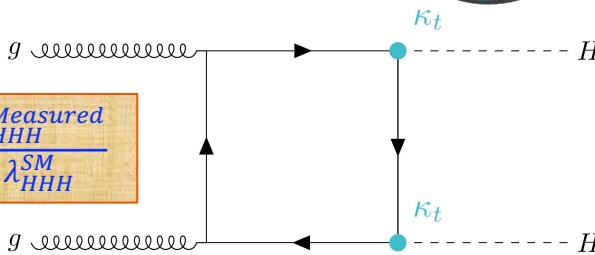
HH production to prob the self coupling λ_{HHH} :

- Leading HH production mode at LHC is gluon-gluon Fusion (ggF):

- $\sigma_{ggF}^{SM} = 31.05 \text{ fb @ NNLO for } \sqrt{s} = 13 \text{ TeV}$

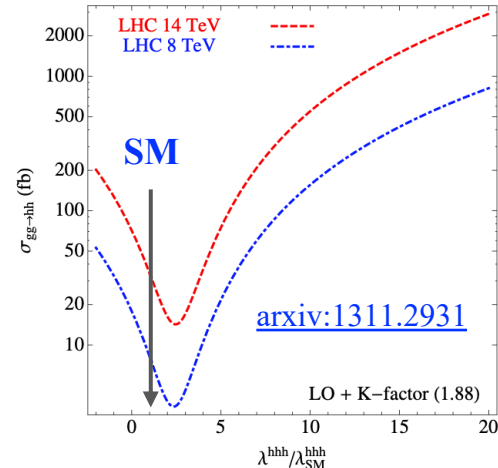
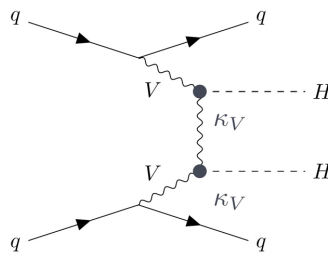
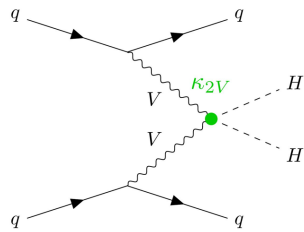
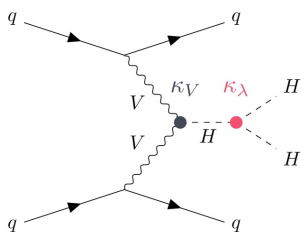


$$\kappa_\lambda = \frac{\lambda_{HHH}^{\text{Measured}}}{\lambda_{HHH}^{\text{SM}}}$$



- Second leading HH production mode is vector-boson-fusion (VBF):

- $\sigma_{ggF}^{SM} = 1.73 \text{ fb @ N3LO for } \sqrt{s} = 13 \text{ TeV}$



Higgs self-coupling measurement in ATLAS

Full run2 140 fb⁻¹

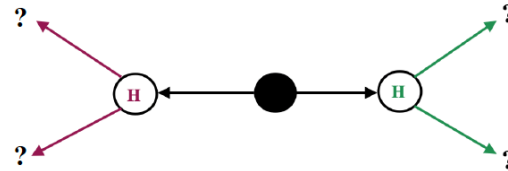
Given that $H \rightarrow bb$ has the highest B.R is mostly exploited by the searches

$bbbb$

- B.R of 34 % the Largest B.R
- Challenging background

$bb\tau\tau$

- B.R of 7.3 % moderate
- Depends on τ decay modes
- Mixed leptonic/hadronic state



	bb	WW	$\tau\tau$	ZZ	$\gamma\gamma$
bb	34%				
WW	25%	4.6%			
$\tau\tau$	7.3%	2.7%	0.39%		
ZZ	3.1%	1.1%	0.33%	0.069%	
$\gamma\gamma$	0.26%	0.10%	0.028%	0.012%	0.0005%

$bb\gamma\gamma$

- Clean $m_{\gamma\gamma}$ peak
- Small B.R of (0.26 %)

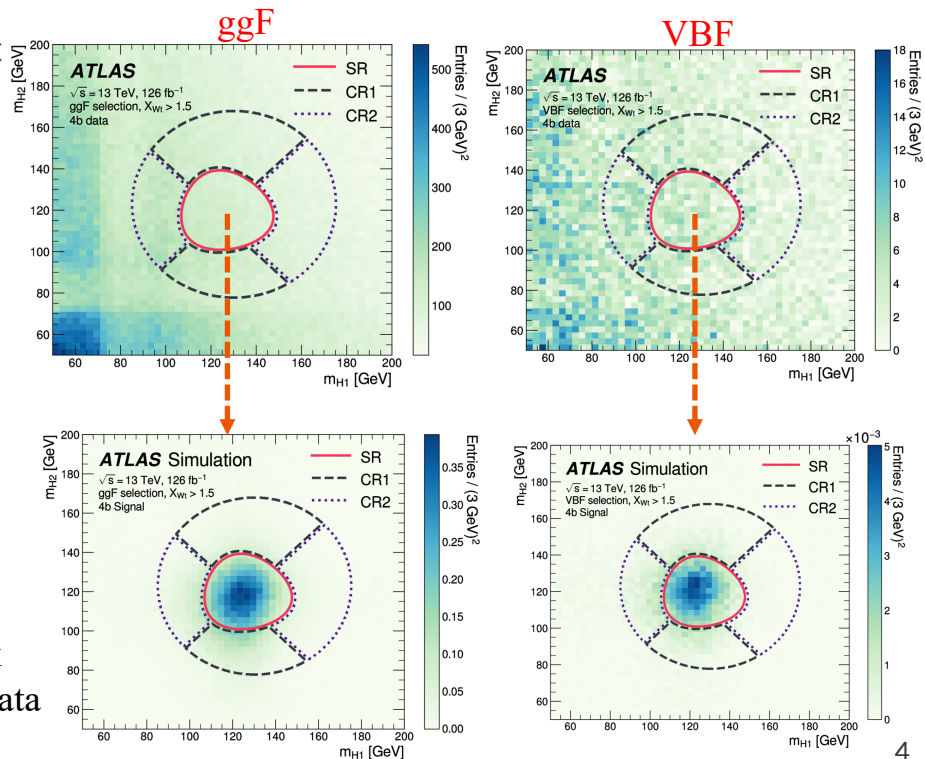
$bb\ell\ell + E_{miss}^T$

- $\ell\ell\nu\nu$ from ($\tau\tau + WW + ZZ$)
- Clean $\ell\ell + E_{miss}^T$

Run2 non-resonant $HH \rightarrow bbbb$ Analysis strategy

[*Phys. Rev. D 108 \(2023\) 052003*](#)

- Due to large QCD the multi-jet background make it challenging to distinguish signal from the background
- Targeting ggF and VBF production modes with dedicated categories based on the presence of additional jets
- Signal regions are defined by the selections in the 2D $m_{H1}:m_{H2}$ plane
- Major backgrounds
 - QCD multi-jets ($\sim 95\%$)
 - $t\bar{t}$ ($\sim 5\%$)
- Total background estimated from data using a neural network trained in control regions to re-weight 2b data to look like 4b data

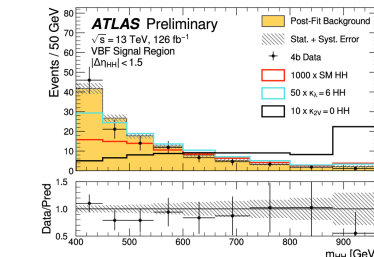
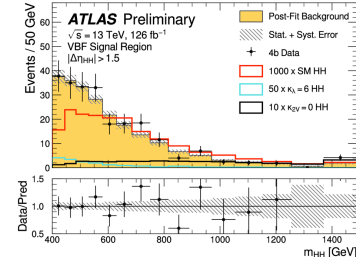
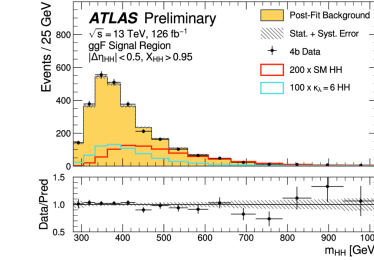
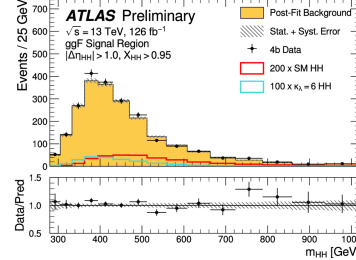
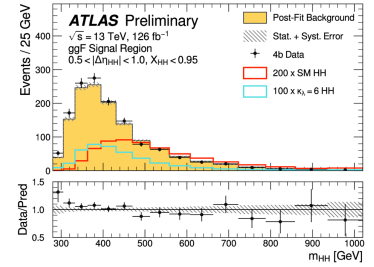
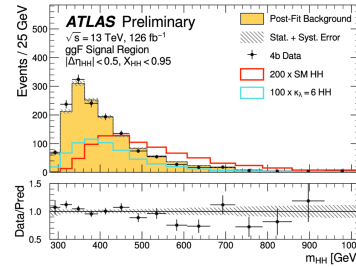


Run2 non-resonant HH \rightarrow bbbb Analysis strategy

Phys. Rev. D 108 (2023) 052003

- Further splitting is performed for ggF and VBF categories to enhance sensitivity to SM signal and to the signals with BSM couplings
- ggF category splitting:
 - 3×2 categories in bins of
 - $|\Delta\eta_{HH}| \times X_{HH}$
- VBF category splitting:
 - 2 categories in bins of
 - $|\Delta\eta_{HH}|$
- Final discriminant variable:
 - m_{HH} is used as final discriminant variable in 8 signal regions

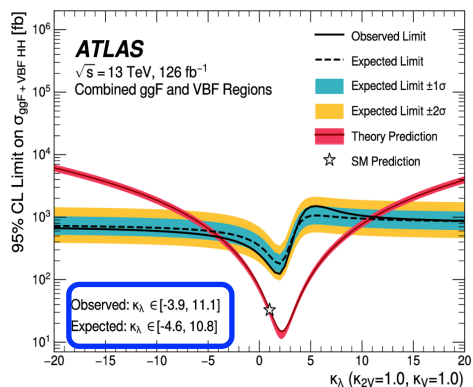
$$X_{HH} = \sqrt{\left(\frac{m_{H1} - 124 \text{ GeV}}{0.1 m_{H1}}\right)^2 + \left(\frac{m_{H2} - 117 \text{ GeV}}{0.1 m_{H2}}\right)^2}$$



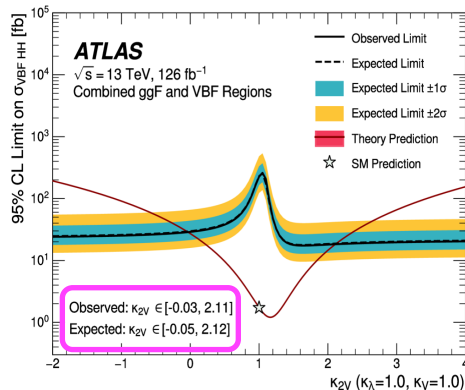
Run2 results non-resonant $HH \rightarrow bbbb$ Analysis

Cross-sectional limits

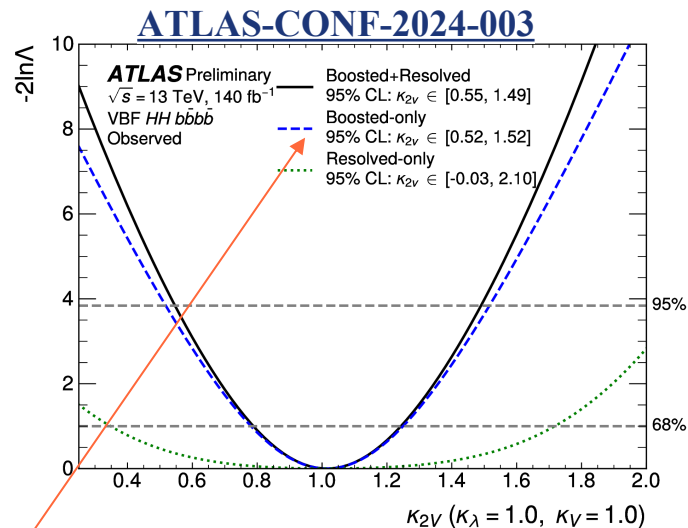
	Observed Limit	-2σ	-1σ	Expected Limit	$+1\sigma$	$+2\sigma$
μ_{ggF}	5.5	4.4	5.9	8.2	12.4	19.6
μ_{VBF}	130	70	100	130	190	280
$\mu_{ggF+VBF}$	5.4	4.3	5.8	8.1	12.2	19.1



Observed: $\kappa_\lambda \in [-3.9, 11.1]$
 Expected: $\kappa_\lambda \in [-4.6, 10.8]$



Observed: $\kappa_{2V} \in [-0.03, 2.11]$
 Expected: $\kappa_{2V} \in [-0.05, 2.12]$



Dedicated boosted HH VBF analysis is performed
 \rightarrow To enhance κ_{2V} sensitivity

Run2 non-resonant $HH \rightarrow bb\tau\tau$ Analysis strategy

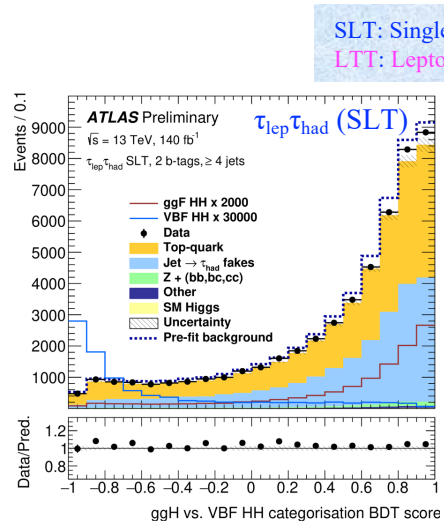
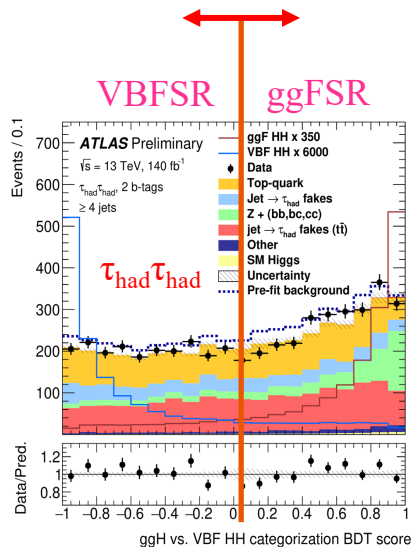
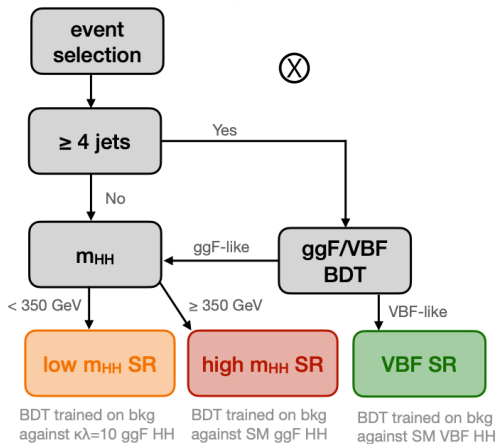
Extended categorization to improve constraints on HHH and HHV coupling

[ATLAS-CONF-2023-071/](#)

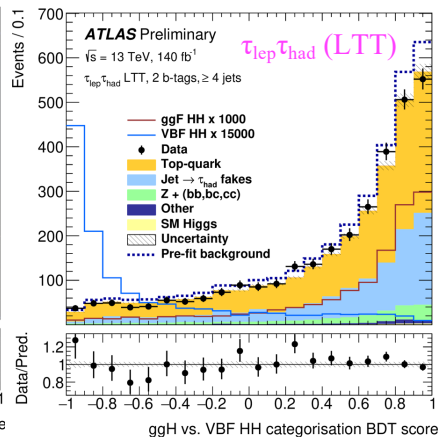
Given the τ decay two sub-channels are considered

- Semi leptonic $\tau_{lep}\tau_{had}$
 - 1 Lepton (e/μ) and 1τ
- Fully hadronic $\tau_{had}\tau_{had}$
 - 2τ

Categorization cut chosen not to penalize k_λ constraint and inclusive HH signal strength limit



SLT: Single lepton Trigger channel
LTT: Lepton+Tau Trigger channel



Run2 non-resonant $HH \rightarrow bb\tau\tau$ Analysis strategy

Main backgrounds:

[ATLAS-CONF-2023-071/](#)

- $t\bar{t}b$
- Z + heavy flavour jets

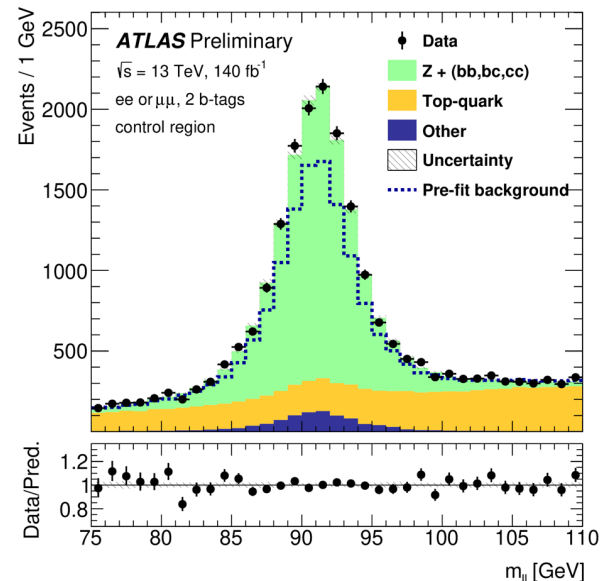
Dedicated control region
[ee or $\mu\mu$, $75 \text{ GeV} < m_{\ell\ell} < 110 \text{ GeV}$
, $m_{bb} < 40 \text{ GeV}$ or $m_{bb} > 210 \text{ GeV}$]

- Single top
- Single Higgs
- Diboson

From simulation

- $t\bar{t}b$ with jet $\rightarrow \tau_{\text{had}}$ fakes
- QCD multijet with jet $\rightarrow \tau_{\text{had}}$ fakes

data-driven
from anti-ID CR extrapolated
into the SR with fake factors



Signal is extracted through a joint fit to all SRs and the CR

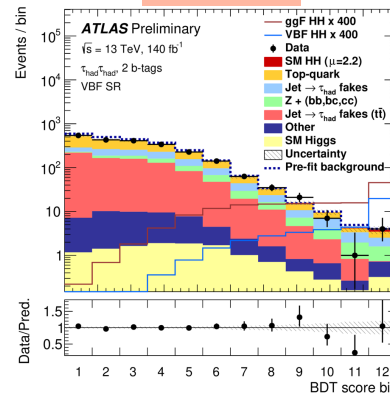
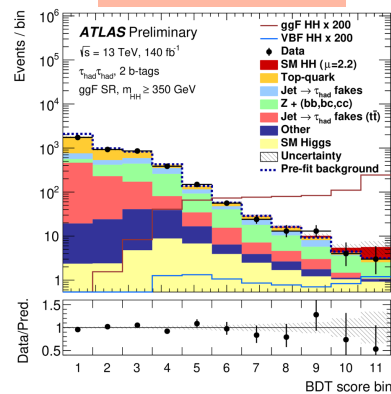
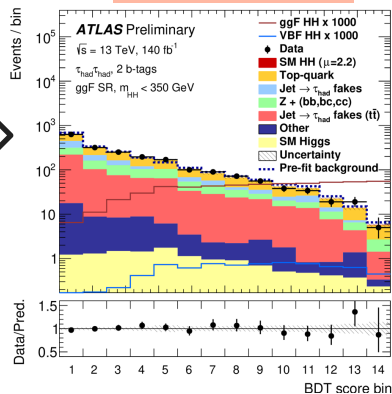
Run2 non-resonant HH \rightarrow bb $\tau\tau$ Analysis strategy

low m_{HH} SR

high m_{HH} SR

VBFSR

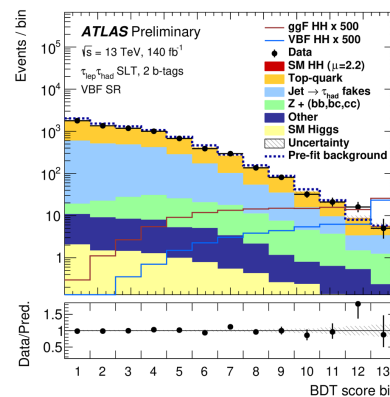
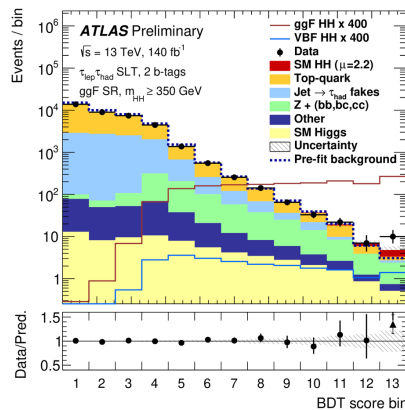
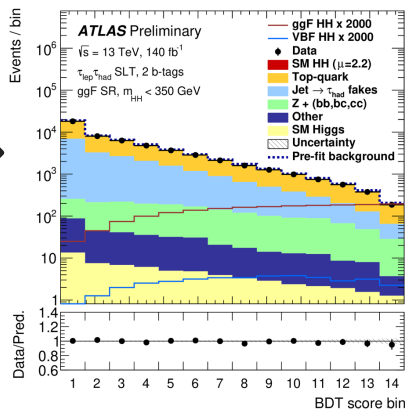
$\tau_{had}\tau_{had}$



[ATLAS-CONF-2023-071/](#)

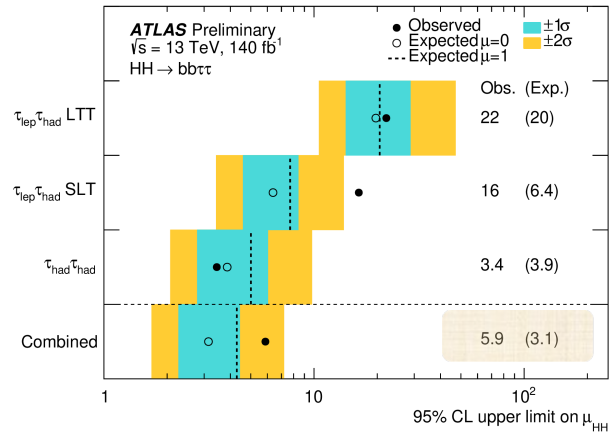
\rightarrow BDT outputs are used as final discriminant

$\tau_{lep}\tau_{had}$ (SLT)

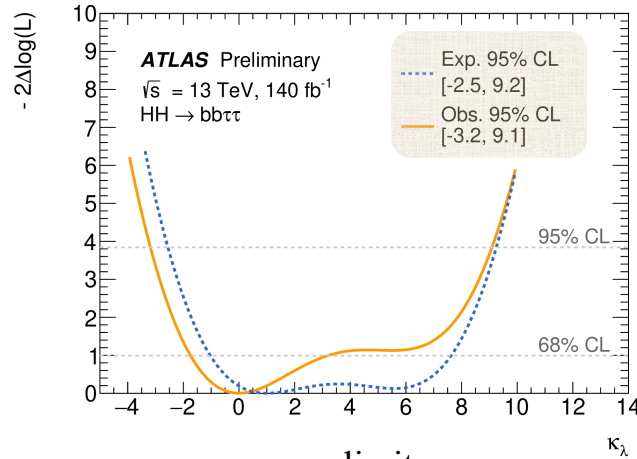


Run2 results non-resonant $HH \rightarrow bb\tau\tau$ Analysis

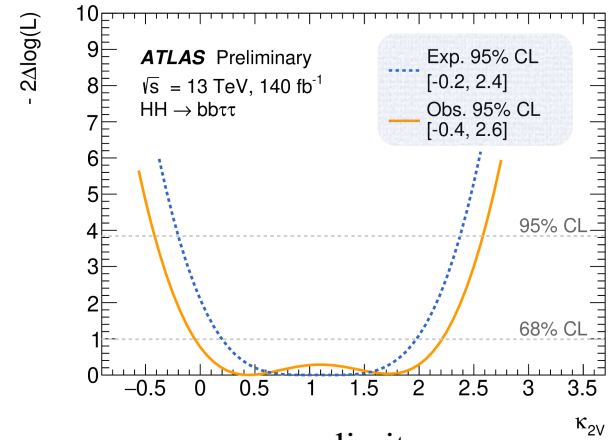
ATLAS-CONF-2023-071



Cross-sectional limits



κ_λ limits



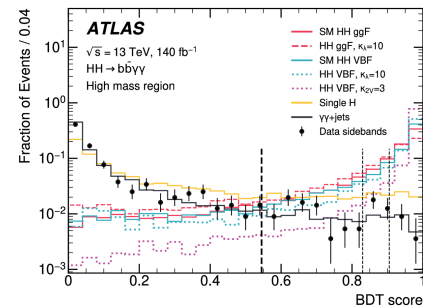
κ_{2V} limits

Run2 non-resonant $HH \rightarrow b\bar{b}\gamma\gamma$ Analysis strategy

Interesting events are selected if they fulfil the selection requirements **targeting** the $b\bar{b}\gamma\gamma$ signature



JHEP 01 (2024) 066

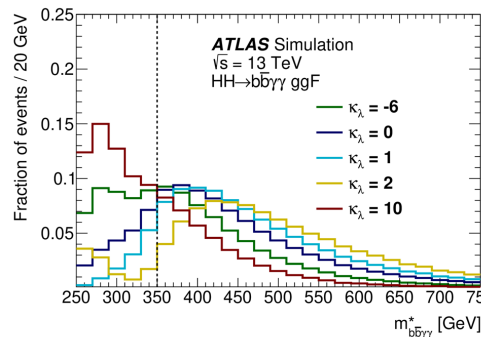


Events in the signal region are then categorized, relying on the **reduced 4-object invariant mass** $m_{b\bar{b}\gamma\gamma}^* = m_{b\bar{b}\gamma\gamma} - (m_{bb} - 125 \text{ GeV}) - (m_{\gamma\gamma} - 125)$ and BDT output

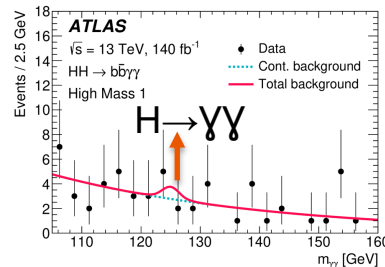
Two bins defined in $m_{b\bar{b}\gamma\gamma}^*$

- **Low mass** region $m_{b\bar{b}\gamma\gamma}^* < 350 \text{ GeV}$

- **High mass** region $m_{b\bar{b}\gamma\gamma}^* > 350 \text{ GeV}$



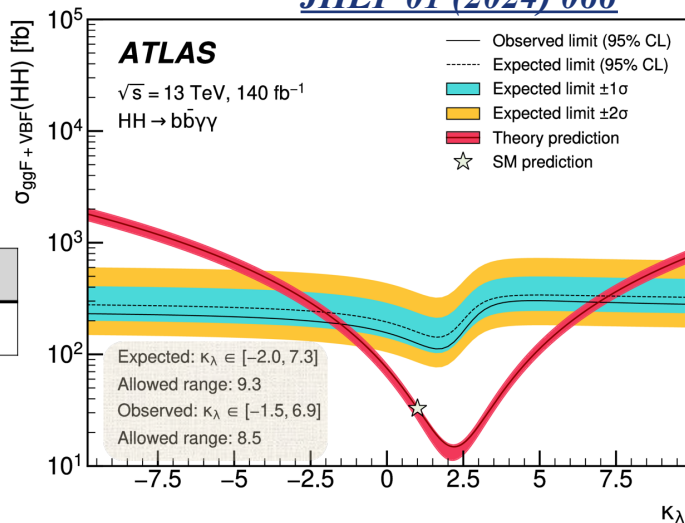
Final Fit discriminant



In events with **more than 4 jets**, the **candidate VBF-jets** are **tagged** via a dedicated **BDT-based classifier**

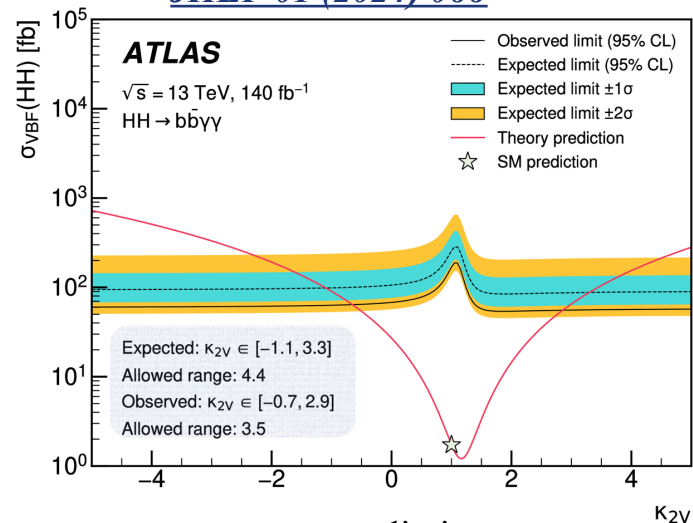
Run2 results non-resonant $HH \rightarrow b\bar{b}\gamma\gamma$ Analysis

JHEP 01 (2024) 066



κ_λ limits

JHEP 01 (2024) 066



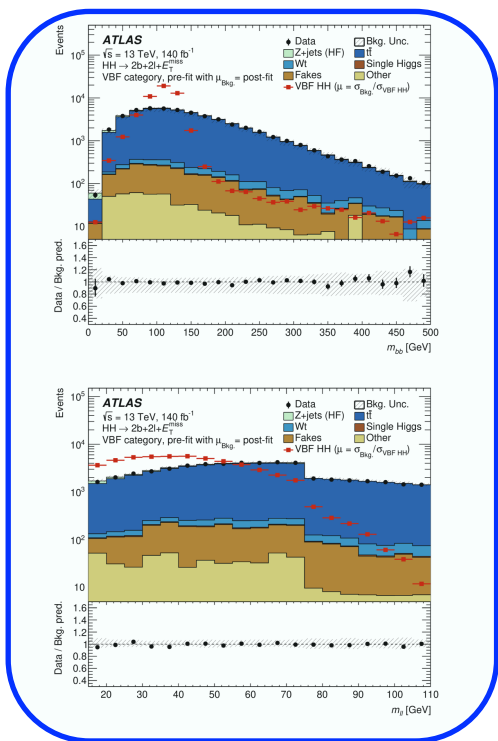
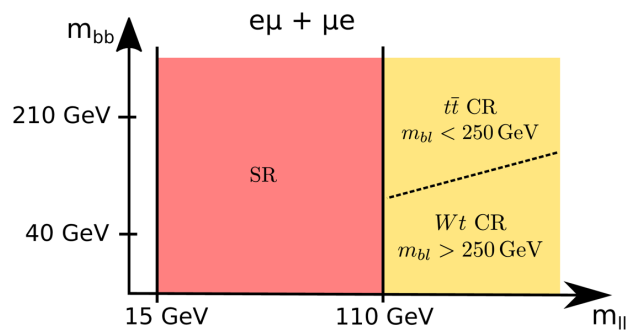
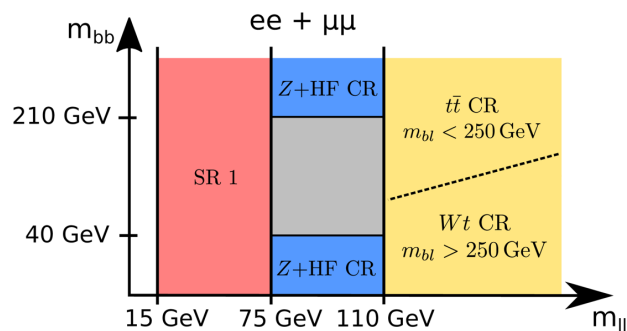
κ_{2V} limits

	Observed	Expected
$\mu(HH)$	4.0	5.0

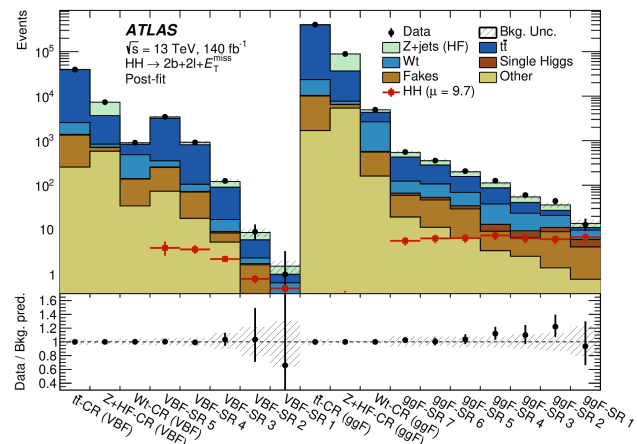
Cross-sectional limits

Run2 non-resonant $bb\ell\ell + E_{miss}^T$

The analysis focuses on the $HH \rightarrow b\bar{b} + WW^*/ZZ^*/\tau^+\tau^- \rightarrow b\bar{b} + \ell^+\ell^- + \text{neutrinos}$



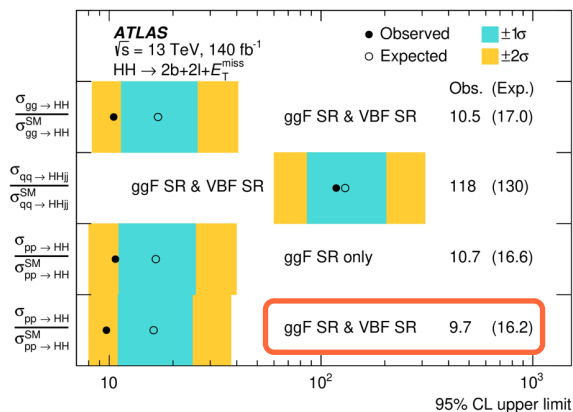
[arXiv:2310.11286](https://arxiv.org/abs/2310.11286)



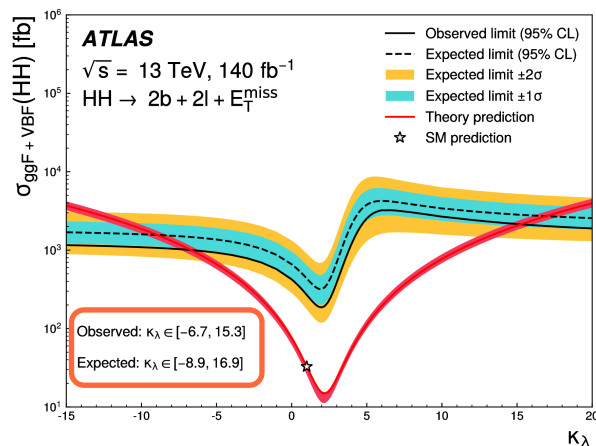
DNN (BDT) bins numbered 1-7(5) by decreasing signal purity

Run2 results non-resonant $bb\ell\ell + E_{miss}^T$

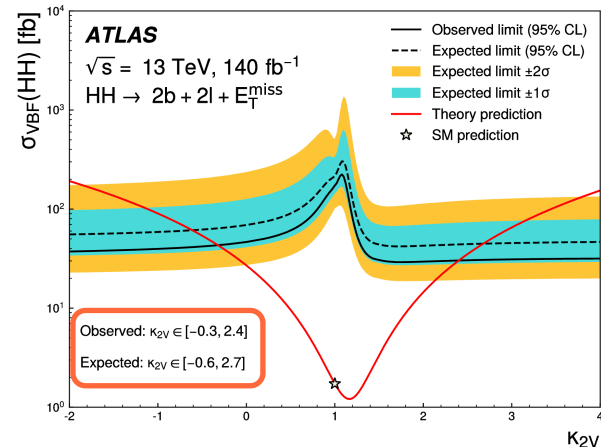
[arXiv:2310.11286](https://arxiv.org/abs/2310.11286)



Cross-sectional limits



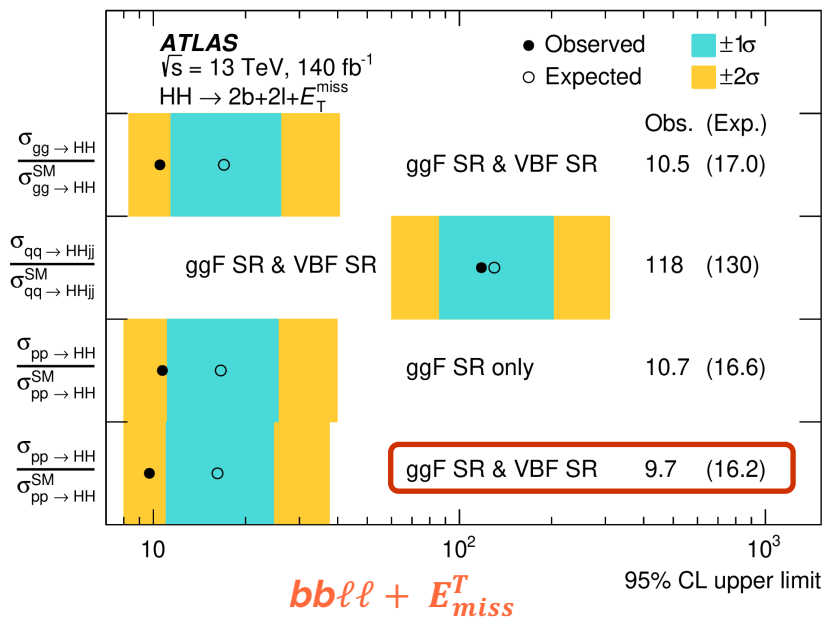
κ_λ limits



κ_{2V} limits

Combine Cross-section limits

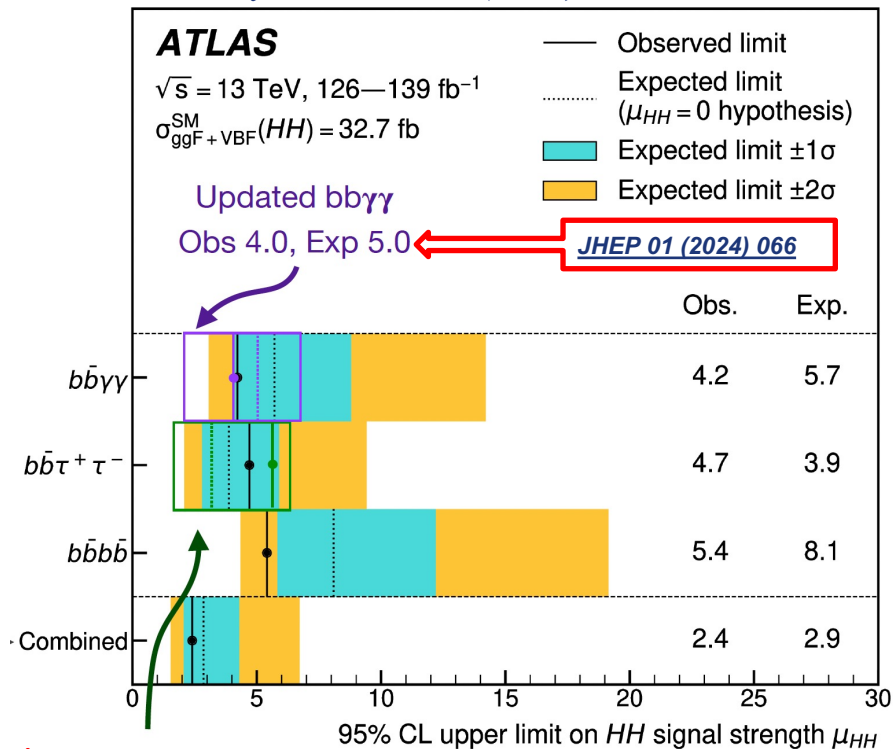
[arXiv:2310.11286](https://arxiv.org/abs/2310.11286)



[ATLAS-CONF-2023-071](#)

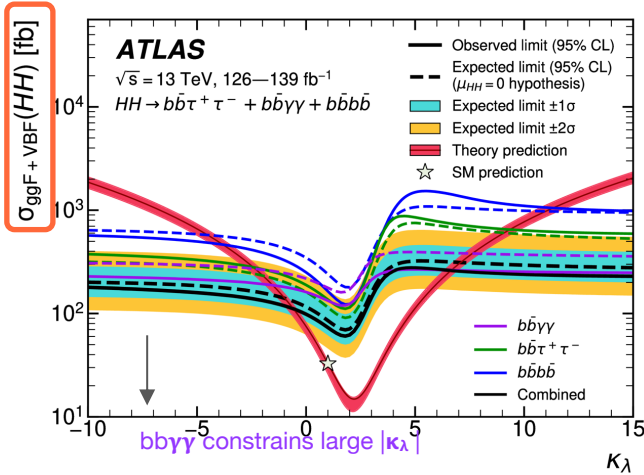
Updated $bb\tau\tau$ Obs 5.9, Exp 3.2

[Phys. Lett. B 843 \(2023\) 137745](#)



Combine Coupling limits

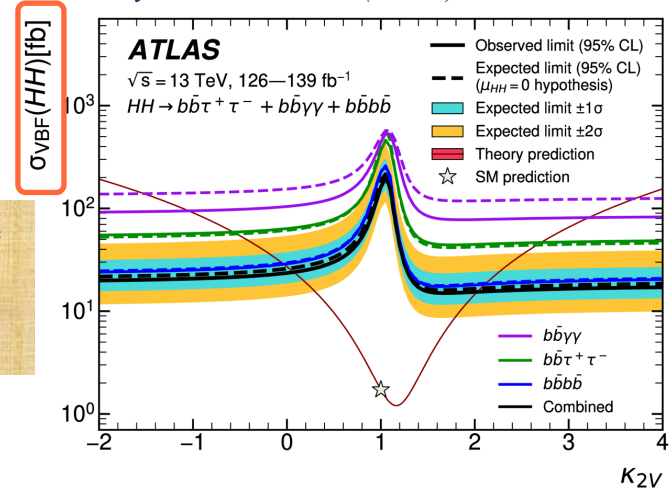
Phys. Lett. B 843 (2023) 137745



The combined results will be computed again for the new re-optimised analysis ($bb\tau\tau$ and $bb\gamma\gamma$)

Final state	Obs. 95% CL	Exp. 95% CL	Obs. value $^{+1\sigma}_{-1\sigma}$
$HH \rightarrow b\bar{b}\gamma\gamma$	$-1.4 < \kappa_\lambda < 6.5$	$-3.2 < \kappa_\lambda < 8.1$	$\kappa_\lambda = 2.8^{+2.0}_{-2.2}$
$HH \rightarrow b\bar{b}\tau^+\tau^-$	$-2.7 < \kappa_\lambda < 9.5$	$-3.1 < \kappa_\lambda < 10.2$	$\kappa_\lambda = 1.5^{+5.9}_{-2.5}$
$HH \rightarrow b\bar{b}b\bar{b}$	$-3.3 < \kappa_\lambda < 11.4$	$-5.2 < \kappa_\lambda < 11.6$	$\kappa_\lambda = 6.2^{+3.0}_{-5.2}$
HH combination	$-0.6 < \kappa_\lambda < 6.6$	$-2.1 < \kappa_\lambda < 7.8$	$\kappa_\lambda = 3.1^{+1.9}_{-2.0}$

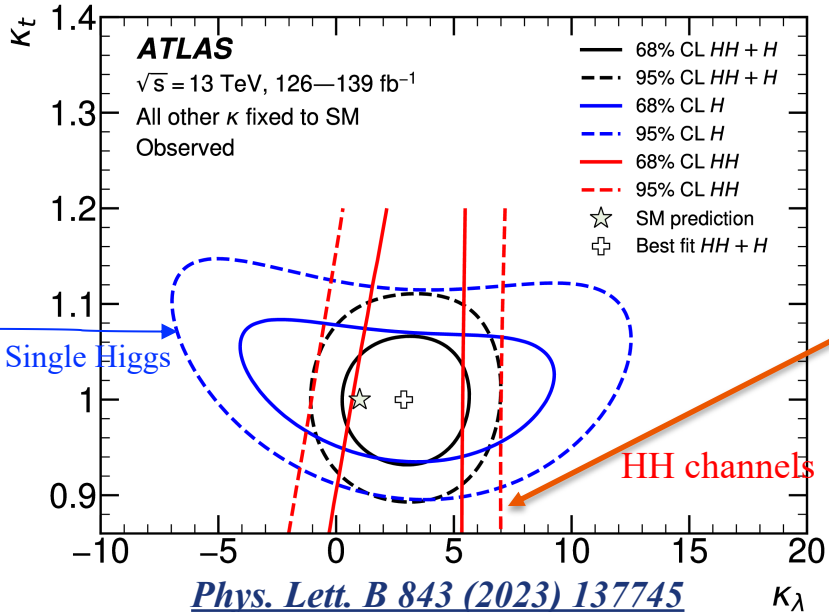
Phys. Lett. B 843 (2023) 137745



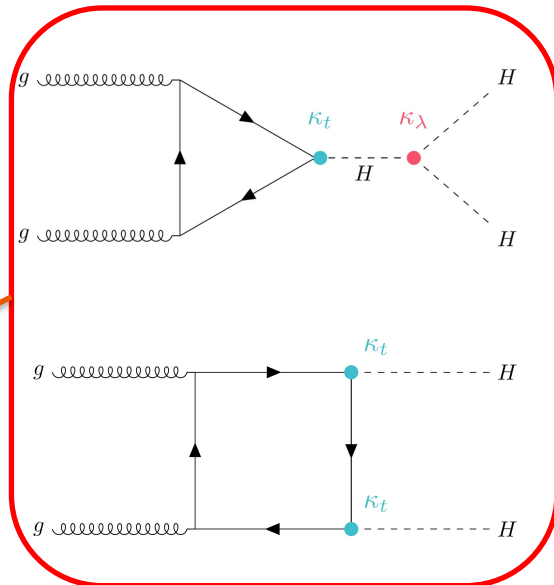
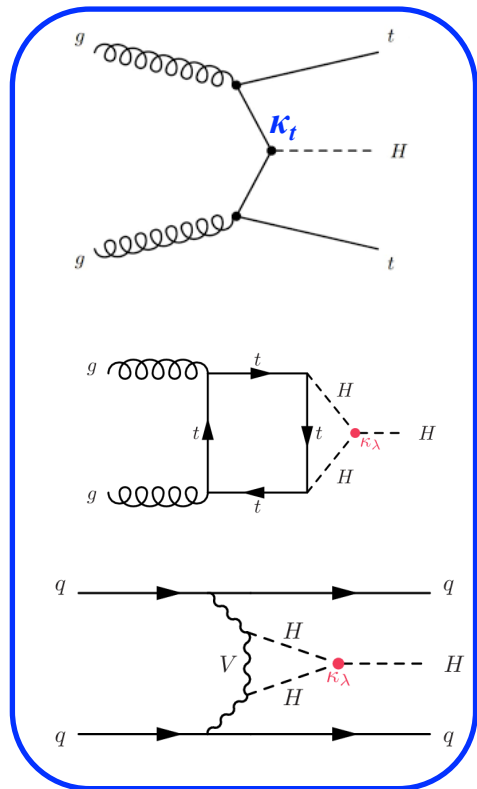
Final state	Obs. 95% CL	Exp. 95% CL	Obs. value $^{+1\sigma}_{-1\sigma}$
$HH \rightarrow b\bar{b}\gamma\gamma$	$-0.8 < \kappa_{2V} < 3.0$	$-1.6 < \kappa_{2V} < 3.7$	$\kappa_{2V} = 1.1^{+1.0}_{-1.0}$
$HH \rightarrow b\bar{b}\tau^+\tau^-$	$-0.6 < \kappa_{2V} < 2.7$	$-0.5 < \kappa_{2V} < 2.7$	$\kappa_{2V} = 1.5^{+0.7}_{-1.7}$
$HH \rightarrow b\bar{b}b\bar{b}$	$0.0 < \kappa_{2V} < 2.1$	$0.0 < \kappa_{2V} < 2.1$	$\kappa_{2V} = 1.0^{+0.7}_{-0.6}$
HH combination	$0.1 < \kappa_{2V} < 2.0$	$0.0 < \kappa_{2V} < 2.1$	$\kappa_{2V} = 1.1^{+0.6}_{-0.6}$

Cross-section limits H and HH combination

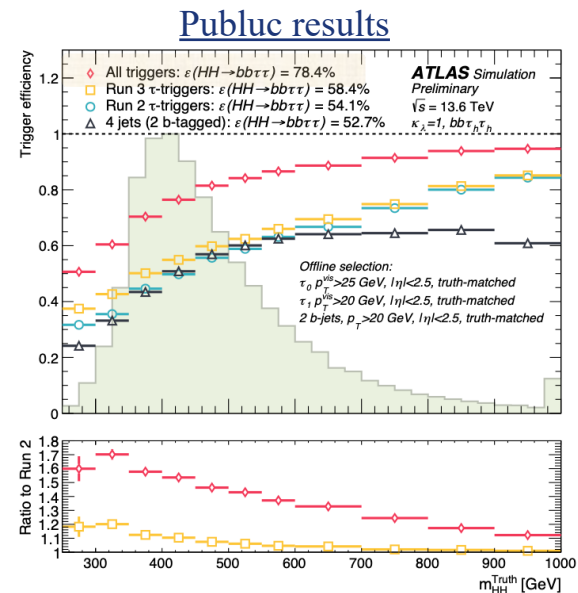
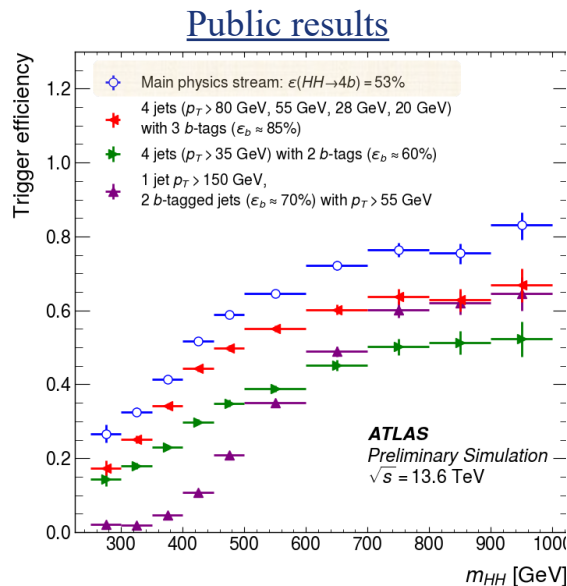
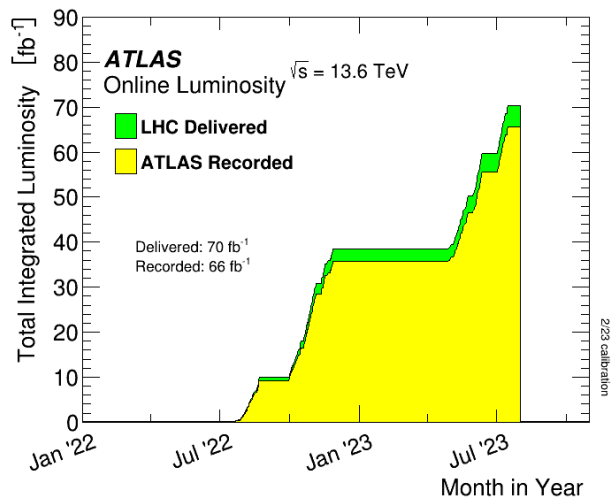
Values outside $-0.4 < \kappa_\lambda = (\lambda_{HHH}/\lambda_{SMHHH}) < 6.3$ are excluded at 95% CL



Constraints in the κ_λ - κ_t plane from single-Higgs (blue) and double-Higgs (red) analyses, and their combination (black)



Towards Run3

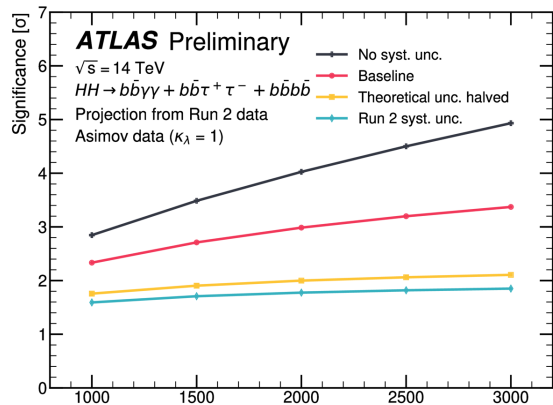


- Trigger improvements in $bbbb$, $bb\tau\tau$: 50% more efficient than Run 2
- Tracking for hadronic signatures \rightarrow Particle Flow jets
- Deep/Graph Neural Net b -taggers
- Optimised event selections, increased bandwidth

Prospects High Luminosity LHC (HL-LHC)

Extrapolations of new ATLAS full run2 non-resonant HH searches in the $b\bar{b}\tau^+\tau^-$ and $b\bar{b}\gamma\gamma$ channels to HL-LHC with 3000 fb^{-1}

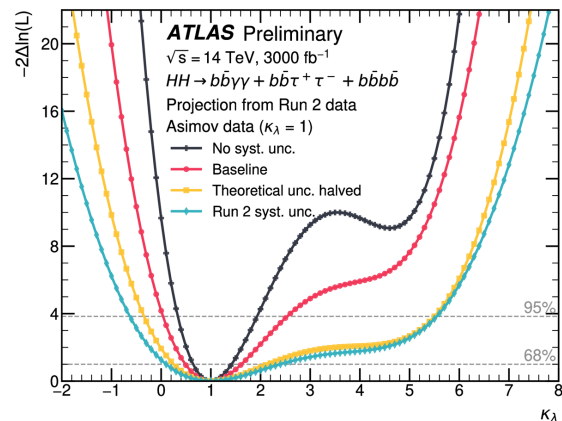
ATL-PHYS-PUB-2022-053



Baseline:
 The systematic uncertainties are adjusted following the latest recommendations from HL-LHC [\[Link\]](#)

Uncertainty scenario	Significance [σ]				Combined signal strength precision [%]
	$b\bar{b}\gamma\gamma$	$b\bar{b}\tau^+\tau^-$	$b\bar{b}b\bar{b}$	Combination	
No syst. unc.	2.3	4.0	1.8	4.9	-21/+22
Baseline	2.2	2.8	0.99	3.4	-30/+33
Theoretical unc. halved	1.1	1.7	0.65	2.1	-47/+48
Run 2 syst. unc.	1.1	1.5	0.65	1.9	-53/+65

ATL-PHYS-PUB-2022-005



Uncertainty scenario	κ_λ 68% CI	κ_λ 95% CI
No syst. unc.	[0.7, 1.4]	[0.3, 1.9]
Baseline	[0.5, 1.6]	[0.0, 2.5]
Theoretical unc. halved	[0.3, 2.2]	[-0.3, 5.5]
Run 2 syst. unc.	[0.1, 2.4]	[-0.6, 5.6]

Conclusion

- HH searches allows to probe directly the Higgs self-coupling
- Active ATLAS searches are ongoing covering most of the channels
 - *Measures many possible decay channels of the HH*
- In combination of the HH decay channels ATLAS has achieved most stringent limits on non-resonant HH production and most stringent constraints on κ_λ until now

The Observed upper limit 2.4 at 95 % CL $-0.6 < \kappa_\lambda < 6.6$ at 95% CL

- New HL-LHC extrapolations based on latest results improved compared to the ones based on the 36 fb^{-1} analysis
 - *Expected more than 3.0σ evidence and 50 % uncertainty on κ_λ for SM HH from ATLAS*

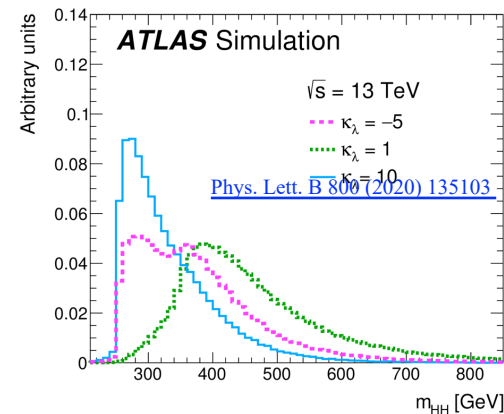
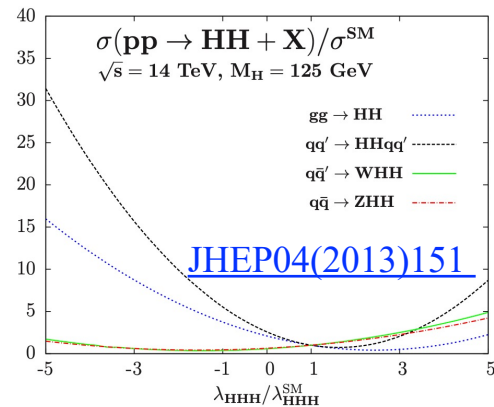
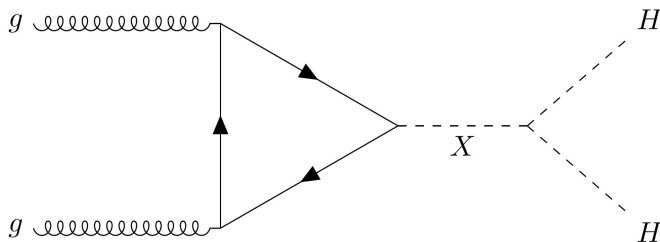
Potential for major gains with a large Run 3 dataset — keep pushing!



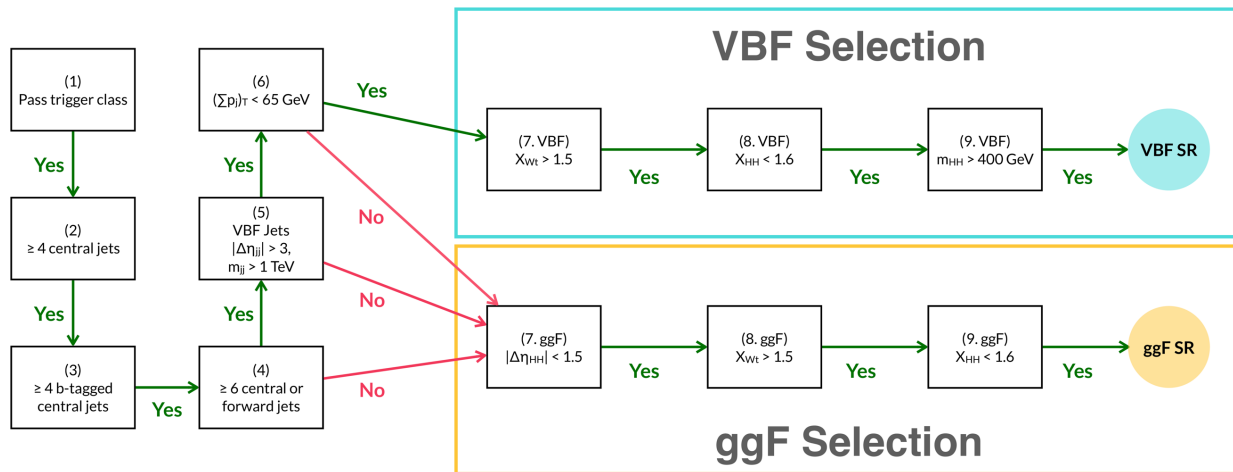
Backup slides

BSM Physics in Higgs pair production

- Higgs pair production in SM is a rare process
 - The production cross-section is 1000 smaller than the single Higgs production
- But still very interesting to study beyond the SM physics (BSM)
- Large variations of non-resonant cross section with modifications of κ_λ for ggF and VBF
 - More than a factor of 2 increase at $\kappa_\lambda = 0$
 - More than a factor of 4 increase at $\kappa_\lambda = -1$
- Modifications of the kinematics of the process with variations of
 - due to different contributions and interference of the Feynman diagrams
- Production of BSM resonances $X \rightarrow HH$
 - Enhances the production rate



4b analysis selections



The values of 124 GeV and 117 GeV in the X_{HH} definition are chosen in accord with the centers of the m_{H1} and m_{H2} distributions for correctly paired signal events from simulation.

$CR1$, are used to derive the reweighting function for the nominal background estimate $CR2$ is used to define a systematic uncertainty related to the reweighting function interpolation into the SR

$$x_{Wt} = \min \left[\sqrt{\left(\frac{m_{jj} - m_W}{0.1m_{jj}} \right)^2 + \left(\frac{m_{jjb} - m_t}{0.1m_{jjb}} \right)^2} \right] \quad X_{HH} = \sqrt{\left(\frac{m_{H1} - 124 \text{ GeV}}{0.1m_{H1}} \right)^2 + \left(\frac{m_{H2} - 117 \text{ GeV}}{0.1m_{H2}} \right)^2}$$

4b analysis background estimations

The background estimation makes use of an alternative set of events, which pass the same b -jet triggers and satisfy all the same selection criteria as the $4b$ events, with one difference: they are required to contain exactly two b -tagged jets. This sample, referred to hereafter as “ $2b$ ”, has about two orders of magnitude more events than the $4b$ sample, hence the presence in it of any $HH \rightarrow b\bar{b}b\bar{b}$ signal is negligible, making it suitable for the background estimation. The jets selected to form the two Higgs boson candidates in the $2b$ events are the two b -tagged jets and the two untagged jets with the highest p_T (excluding the VBF jets in the VBF categories).

The kinematic properties of the $2b$ and $4b$ events are not expected to be identical, partly due to different processes contributing to the two samples, but also due to differences in the trigger acceptance and because the performance of b -tagging varies as a function of jet p_T and η . Therefore, a reweighting function is required, which, when applied to the $2b$ events, maps their kinematic distributions onto the corresponding $4b$ distributions. This function is derived using the $2b$ and $4b$ events in a *control region* (CR) surrounding the SR in the reconstructed (m_{H1}, m_{H2}) plane and then applied to the $2b$ events in the SR to produce the background estimate. The “inner edge” of the CR is defined by $X_{HH} = 1.6$ and the “outer edge” by:

$$\sqrt{(m_{H1} - 1.05 \cdot 124 \text{ GeV})^2 + (m_{H2} - 1.05 \cdot 117 \text{ GeV})^2} = 45 \text{ GeV} . \quad (3)$$

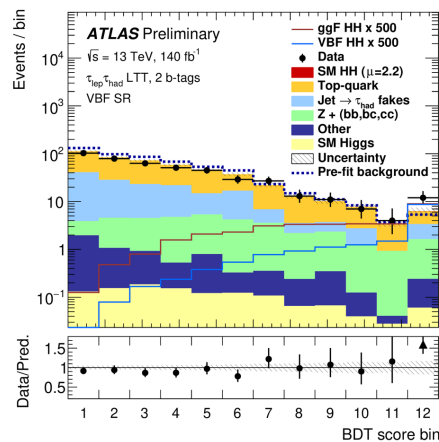
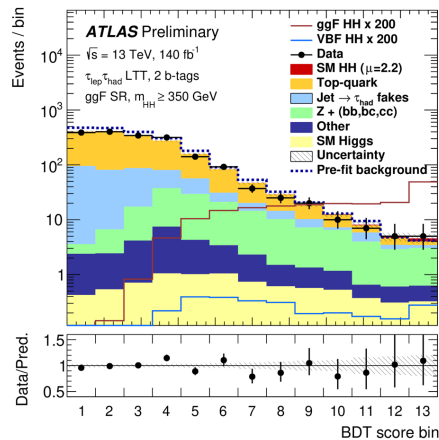
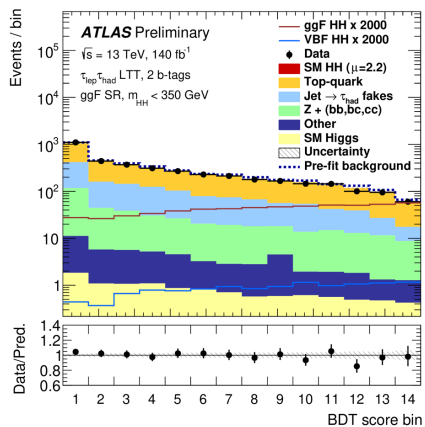
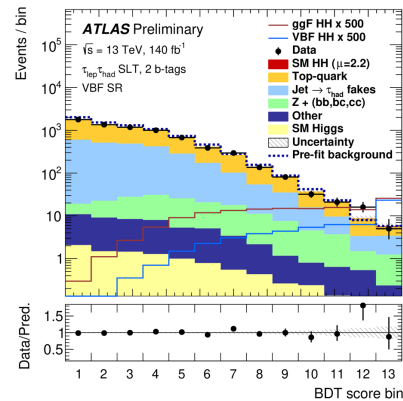
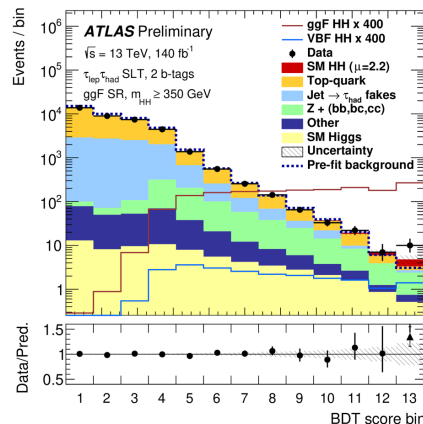
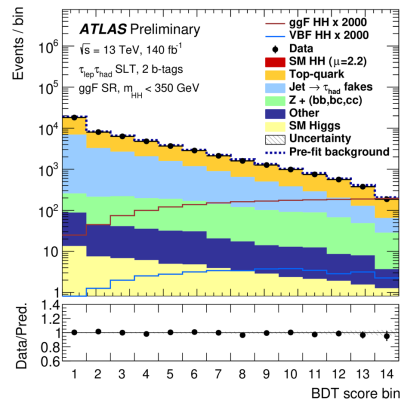
bb $\tau\tau$ kinematic variables

Table 2: Input variables for the categorisation BDTs in each of the three SRs. The superscripts a and c specify the selection of jets that are taken into account for the calculation in addition to the two τ -lepton candidates and \vec{p}_T^{miss} . For variables with a c , only the four-momenta of central jets, i.e. jets with $|\eta| < 2.5$, are included, while an a indicates that all available jets are included.

Variable	$\tau_{\text{had}}\tau_{\text{had}}$	$\tau_{\text{lep}}\tau_{\text{had}}$ SLT	$\tau_{\text{lep}}\tau_{\text{had}}$ LTT
m_{jj}^{VBF}	✓	✓	✓
$\Delta\eta_{jj}^{\text{VBF}}$	✓	✓	✓
VBF $\eta_0 \times \eta_1$	✓	✓	
$\Delta\phi_{jj}^{\text{VBF}}$	✓		
$\Delta R_{jj}^{\text{VBF}}$		✓	✓
$\Delta R_{\tau\tau}$	✓		
m_{HH}	✓		
f_2^a	✓		
C^a		✓	✓
m_{Eff}^a		✓	✓
f_0^c		✓	
f_0^a			✓
h_3^a			✓

bb τ BDT

Single lepton trigger Channel

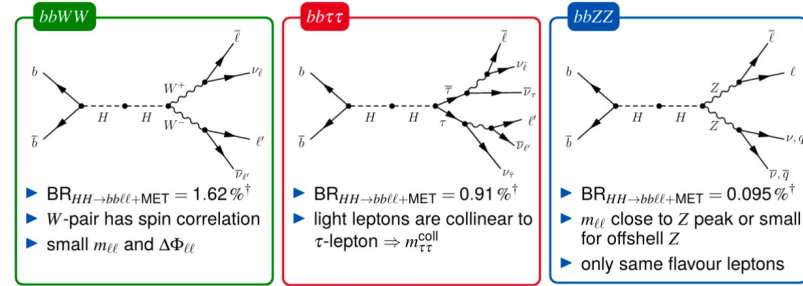


Lepton + τ_{had} trigger

$bb\ell\ell + E_{miss}^T$ pre-selections

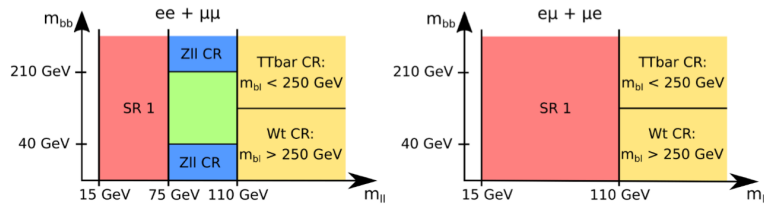
Preselection:

- Single and dilepton triggers
- Exactly two light opposite charge $p_T > 9$ GeV leptons
- Exactly two $p_T > 20$ GeV DL1r (77 % WP) b -tagged jets



Gluon-gluon fusion:

- Veto VBF selection in SR1
- Use NN score as final discriminant



Vector boson fusion:

- ≥ 2 additional $p_T > 30$ GeV jets with
 - $\max(\Delta\eta_{jj}) > 4$
 - $\max(m_{jj}) > 600$ GeV
- Use BDT score as final discriminant
- Separate control regions for ggF and VBF signal regions
- Non-prompt lepton fakes estimated with data-driven method

bbℓℓ + E_{miss}^T MVA inputs

Input feature	Description
same flavour	unity if final state leptons are ee or μμ, zero otherwise
p_T^ℓ, p_T^b	transverse momenta of the leptons, <i>b</i> -tagged jets
$m_{\ell\ell}, p_T^{\ell\ell}$	invariant mass and the transverse momentum of the di-lepton system
m_{bb}, p_T^{bb}	invariant mass and the transverse momentum of the <i>b</i> -tagged jet pair system
m_{T2}^{bb}	transverse mass of the two <i>b</i> -tagged jets
$\Delta R_{\ell\ell}, \Delta R_{bb}$	ΔR between the two leptons and two <i>b</i> -tagged jets
$m_{b\ell}$	$\min\{\max(m_{b_0\ell_0}, m_{b_1\ell_1}), \max(m_{b_0\ell_1}, m_{b_1\ell_0})\}$
$\min \Delta R_{b\ell}$	minimum ΔR of all <i>b</i> -tagged jet and lepton combinations
$m_{bb\ell\ell}$	invariant mass of the <i>bbℓℓ</i> system
$E_T^{\text{miss}}, E_T^{\text{miss-sig}}$	missing transverse energy and its significance
$m_T(\ell_0, E_T^{\text{miss}})$	transverse mass of the <i>p_T</i> -leading lepton with respect to E_T^{miss}
$\min m_{T,\ell}$	minimum value of $m_T(\ell_0, E_T^{\text{miss}})$ and $m_T(\ell_1, E_T^{\text{miss}})$
H_{T2}^R	measure for boostedness ¹ of the two Higgs bosons

DNN (ggF)

Input feature	Description
$\eta_{\ell_0}, \eta_{\ell_1}, \phi_{\ell_0}, \phi_{\ell_1}, p_T^{\ell_0}, p_T^{\ell_1}$	η, ϕ, p_T of the <i>p_T</i> -(sub)leading lepton
$\eta_{b_0}, \eta_{b_1}, \phi_{b_0}, \phi_{b_1}, p_T^{b_0}, p_T^{b_1}$	η, ϕ, p_T of the <i>p_T</i> -(sub)leading <i>b</i> -tagged jet
$\eta_{j_0}, \eta_{j_1}, \phi_{j_0}, \phi_{j_1}, p_T^{j_0}, p_T^{j_1}$	ϕ, η, p_T of the <i>p_T</i> -(sub)leading non <i>b</i> -tagged jet
$E_T^{\text{miss}}, \phi_{E_T^{\text{miss}}}, E_T^{\text{miss-sig}}$	missing transverse energy, its ϕ and significance
$p_T^{bb}, \Delta R_{bb}, \Delta\phi_{bb}, m_{bb}$	$p_T, \Delta R, \Delta\phi$ and invariant mass of di- <i>b</i> -jet system
$p_T^{\ell\ell}, \Delta R_{\ell\ell}, \Delta\phi_{\ell\ell}, m_{\ell\ell}, \phi_{\text{centrality}}^{\ell\ell}$	$p_T, \Delta R, \Delta\phi, p_T$ and centrality ¹ of di-leptons system
$p_T^{bb\ell\ell}, m_{bb\ell\ell}$	p_T and invariant mass of the <i>bbℓℓ</i> system
$p_T^{bb\ell\ell+E_T^{\text{miss}}}, m_{bb\ell\ell+E_T^{\text{miss}}}$	p_T and invariant mass of <i>bbℓℓ</i> + E_T^{miss} system
$m_{\ell\ell+E_T^{\text{miss}}}, m_{bb\ell\ell+E_T^{\text{miss}}}$	invariant mass of di-lepton + E_T^{miss} system
$p_T^{E_T^{\text{miss}}+\ell\ell}, \Delta\phi_{E_T^{\text{miss}},\ell\ell}$	p_T of and $\Delta\phi$ between E_T^{miss} and di-lepton system
p_T^{tot}	p_T of <i>bbℓℓ</i> + E_T^{miss} + <i>p_T</i> -leading and -sub-leading jet
m_{tot}	invariant mass of <i>bbℓℓ</i> + E_T^{miss} + <i>p_T</i> -leading and -sub-leading jet
$m_{\text{t}}^{\text{KLF}}$	Kalman fitter top-quark mass
$\min \Delta R_{\ell_0 j}, \min \Delta R_{\ell_1 j}$	minimum ΔR between <i>p_T</i> -(sub)leading ℓ - <i>j</i> couples
$\sum m_{\ell j}$	sum of the invariant masses of all ℓ +jet combinations
$\max p_T^{ij}, \max m_{jj}$	maximum <i>p_T</i> and invariant mass of any two non <i>b</i> -tagged jets
$\max \Delta\eta_{jj}, \max \Delta\phi_{jj}$	maximum $\Delta\eta$ and $\Delta\phi$ between any two non <i>b</i> -tagged jets
$\min \Delta R_{b\ell}$	minimum ΔR of all <i>b</i> -tagged jet and lepton combinations
$N_{\text{forward jets}}, N_j$	number of forward jets, number of non <i>b</i> -tagged jets
m_{T2}^{bb}	transverse mass of the two <i>b</i> -tagged jets
m_{coll}	collinear mass (reconstruction of $m_{\tau\tau}$)
m_{MMC}	value of the MMC algorithm (reconstruction of $m_{\tau\tau}$)

BDT (VBF)

Resonant HH combination with full Run 2 data

- Searches are performed for BSM resonant HH production: resonance mass point $\in [0.25, 5]$ TeV
- $X \rightarrow HH \rightarrow bbbb, bb\tau\tau, bb\gamma\gamma$
- Similar baseline event selections and background estimations to the non-resonant searches in the same final states
- Optimised signal region selections and discriminants specifically for the resonant signals

Complementarity of searches in different decay channels:

- $bb\gamma\gamma$ [[Phys. Rev. D 106 \(2022\) 052001](#)]
- $bb\tau\tau$ [[JHEP 07 \(2023\) 040](#)]
- $bbbb$ [[Phys. Rev. D 105 \(2022\) 092002](#)]

